FC
422

Chemical Geology, 23 (1978) 239—254

© Elsevier Scientific Publishing Company, Amsterdam — Printed in The Netherlands

UNIVERSITY OF UTAH
RESEARCH INSTITUTE
EARTH SCIENCE LAB.

GL03695

POSSIBLE CATION BUFFERING IN CHLORIDE-RICH GEOTHERMAL WATERS

NAOTATSU SHIKAZONO

Geological Institute, Faculty of Sciences, University of Tokyo, Tokyo 113 (Japan)

(Received May 9, 1977; revised and accepted December 21, 1977)

ABSTRACT

Shikazono, N., 1978. Possible cation buffering in chloride-rich geothermal waters. Chem. Geol., 23: 239—254.

It is theoretically considered that the concentration of alkali and alkali-earth elements in chloride-rich hydrothermal solutions in equilibrium with natural mineral assemblages increases with increasing Cl^- concentration. On a logarithmic cation—Cl^- concentration diagram this relation is shown by a nearly straight line. Analytical data for Na^+, K^+, Li^+, Cs^+, Rb^+, H^+, Ca^{2+}, and Mg^{2+} in geothermal waters and inclusion fluids of high temperature (200—300° C) appear to be generally consistent with the theoretical consideration. The concentrations of Sr^{2+} and Ba^{2+} in low-temperature (50—100° C) Japanese hot springs are characterized by: (1) they are controlled by the concentrations of both dominant monovalent and divalent cations and silicate minerals, or (2) they are controlled by sulfate (such as barite) minerals.

INTRODUCTION

Many studies have recently been made of the chemical composition of geothermal waters and of alteration assemblages in geothermal areas. These studies have shown that the chemical composition of the geothermal waters is intimately related both to the alteration assemblages of host rocks and to temperature. For example, the correlation between the Na/K ratio in geothermal water and temperature has been interpreted as indicating that this ratio is controlled by albite and K-feldspar (White, 1965; Ellis, 1969, 1970). It was pointed out by Ellis (1969, 1970) that the concentrations of not only Na^+ and K^+, but also of other cations such as H^+, Ca^{2+} and Mg^{2+} are largely dependent on the mineral assemblages found in the geothermal area. Ellis (1970) derived the relation between cation concentrations and temperature, assuming that chemical equilibrium is established between the solution and the alteration minerals. Shikazono (1976) proposed a logarithmic cation—Cl^- concentration diagram in order to consider the relation of the concentrations of Na^+, K^+, and Ca^{2+} with Cl^- in solution. The variation in the concentrations of these species with temperature was considered by Fournier and

Truesdell (1973), who used the observed relations to define a Na—K—Ca geothermometer.

In this paper a relation is derived between the concentrations of alkali and alkali earth in a hydrothermal solution in equilibrium with a given mineral assemblage and the Cl^- concentration of the solution at constant temperature. The theoretically predicted results are then compared with the composition of natural geothermal waters and inclusion fluids on logarithmic cation—Cl^- concentration diagrams.

ALTERATION MINERALS IN GEOTHERMAL AREA

Several studies of geothermal areas have shown that alteration assemblages regularly change with increasing depth and temperature. These changes have been observed in Hveragerdi, Iceland (Sigvaldason, 1959, 1967); Reykjanes, Iceland (Björnsson et al., 1970; Tomasson and Kristmannsdóttir, 1972); Otaka, Japan (Yamasaki et al., 1968; Hayashi, 1973); Broadland, New Zealand (Brown and Ellis, 1970); Wairakei, New Zealand (Steiner, 1953, 1968, 1970); and in other areas. According to these studies the following minerals are commonly found at the greatest depth in areas of relatively high temperature (200—300°C): albite, K-feldspar, muscovite, quartz, chlorite, calcite, wairakite, epidote and anhydrite. Pumpellyite and prehnite are mainly found in those areas in which the host rocks for the geothermal area are composed of basic rocks, as in the case at Hveragerdi (Sigvaldason, 1959, 1967) and Reykjanes (Björnsson et al., 1970; Tomasson and Kristmannsdóttir, 1972). Minor occurrences of other minerals such as siderite, magnetite, hematite and tremolite have been reported from some areas. As the thermochemical data of wairakite and epidote at high temperatures are still uncertain, for the purposes of the present study, it is assumed that the minerals in equilibrium with geothermal waters are albite, K-feldspar, muscovite, quartz, calcite, anhydrite and chlorite.

THEORETICAL CONSIDERATIONS

Relation between the concentration of elements and Cl^- in monovalent cation and Cl^- dominant solutions

In geothermal waters the condition of electroneutrality must be fullfilled:

$$\Sigma\, z_{ci} \cdot m_{ci} = \Sigma\, z_{aj} \cdot m_{aj} \qquad (1)$$

In this equation z_{ci} and m_{ci} refer, respectively, to the charge and molality of cation i, and z_{aj} and m_{aj} to the charge and molality of anion j.

Na^+ concentration. It is found in geothermal waters of high temperature (200—300°C) and in inclusion fluids that Na^+ and Cl^- are the predominant cation and anion. If the concentrations of the other species are very low compared with those of Na^+ and Cl^-, eq. 1 is approximated by the

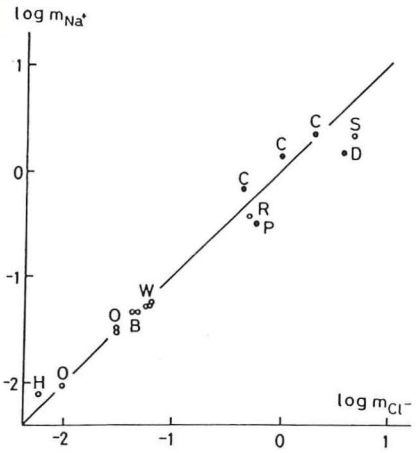

Fig.1. Relation between the Na^+ and Cl^- concentrations of geothermal waters and of inclusion fluids. The *solid line* indicates the condition of electroneutrality approximated by the equation $m_{Na^+} = m_{Cl^-}$. *Solid* and *open circles* mean the chemical analytical data on inclusion fluids and geothermal waters, respectively.
Abbreviations: S = Salton Sea (Muffler and White, 1969); R = Reykjanes (Björnsson et al., 1970); W = Wairakei (Ellis, 1970); B = Broadland (Mahon and Finlayson, 1972); O = Otake (Hayashida and Ejima, 1970; Koga, 1970); H = Hveragerdi (Ellis, 1969); C = Climax (Hall et al., 1974); D = Darwin (Rye et al., 1974); P = Providencia (Rye and Hafftty, 1969).

following equation:

$$m_{Na^+} = m_{Cl^-} \tag{2}$$

Therefore, on a $\log(m_{Na^+})$—$\log(m_{Cl^-})$ diagram, the condition of electroneutrality is approximated by a straight line having a slope of +1 (Fig.1). In Fig.1, data on Na^+ and Cl^- concentrations of some geothermal waters are also plotted. The relation between the natural data and theoretical line will be discussed later.

K^+ concentration. Albite and K-feldspar are commonly observed to coexist in geothermal areas, especially in the deeper and high-temperature regions. If the following reaction is in equilibrium:

$$\text{K-feldspar} + Na^+ \rightleftharpoons \text{albite} + K^+ \tag{3}$$

the equilibrium constant, K_3, is expressed as:

$$K_3 = (a_{Ab} \cdot a_{K^+})/(a_{Kf} \cdot a_{Na^+}) \tag{3a}$$

in which a refers to the activity of the specified species.

Combining eq. 3a with eq. 2, we obtain:

$$\log(m_{K^+}) = \log(m_{Cl^-}) + \log(c_1) \tag{4}$$

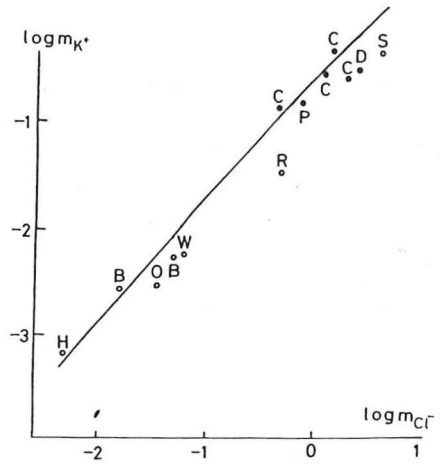

Fig.2. Relation between the K^+ and Cl^- concentrations of geothermal waters and inclusion fluids. The *solid line* defines the equilibrium condition between the solution and the assemblage albite—K-feldspar at 250° C. For symbols used see caption to Fig.1.

in which c_1 equals $(\gamma_{Na^+} \cdot a_{Kf} \cdot K_3)/(\gamma_{K^+} \cdot a_{Ab})$ and γ_i is the activity coefficient of the ith species. In a plot of $\log(m_{K^+})$ vs. $\log(m_{Cl^-})$ (Fig.2) a slope of about +1 is obtained.

Fig.2 was constructed using a K_3 value at 250°C extrapolated from high-temperature data experimentally determined by Orville (1963), Iiyama (1965) and Hemley (1967). Ion activity coefficients were computed using the extended Debye-Hückel equation proposed by Helgeson (1969). The values of effective ionic radius were taken from Garrels and Christ (1965). In the calculation of ion activity coefficients, ionic strength is regarded as $0.5\ (m_{Na^+} + m_{Cl^-})(= m_{Cl^-})$. The activity ratio a_{Kf}/a_{Ab} is assumed to be unity.

Cs^+, Rb^+ and Li^+ concentrations. As in the case of K^+, if the concentrations of alkali elements are controlled by feldspars, it is convenient to take into account the following exchange reaction:

$$\text{albite} + X^+ \rightleftharpoons XAlSi_3O_8 + Na^+ \qquad (5)$$

in which X denotes an alkali element.

The equilibrium constant of eq. 5 is:

$$K_5 = (a_{XAlSi_3O_8} \cdot a_{Na^+})/(a_{Ab} \cdot a_{X^+}) \qquad (5a)$$

From eqs. 5a and 2 we obtain:

$$\log(m_{X^+}) = \log(m_{Cl^-}) + \log(c_2) \qquad (6)$$

in which $c_2 = (a_{XAlSi_3O_8} \cdot \gamma_{Na^+} \cdot K_5)/(a_{Ab} \cdot \gamma_{X^+})$

The concentrations of Li, Rb and Cs in feldspars in geothermal areas have not been studied. However, if the concentration ranges are similar to those

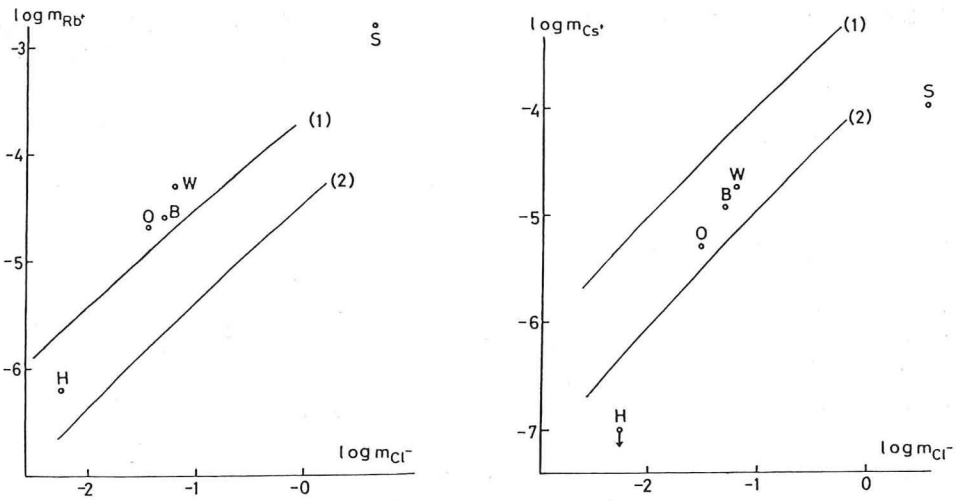

Fig. 3. Relation between the Rb^+ and Cl^- concentrations of geothermal waters. *Solid lines 1* and *2* indicate the equilibrium condition between feldspars and solution, assuming that the Rb content of the feldspar is between 10^{-1} wt.% and 10^{-2} wt.%. For symbols used see caption to Fig.1.

Fig. 4. Relation between the Cs^+ and Cl^- concentrations of geothermal waters. *Solid lines 1* and *2* indicate the equilibrium condition between feldspars and solution, assuming that the Cs content of the feldspar is between 10^{-3} and 10^{-4} wt.% For symbols used see caption to Fig.1.

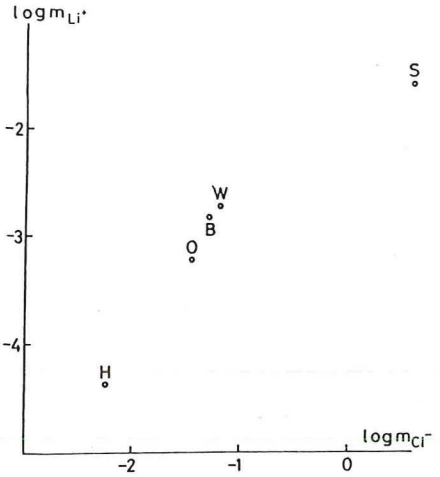

Fig.5. Relation between the Li^+ and Cl^- concentrations of geothermal waters. For symbols used see caption to Fig.1.

observed for feldspars in common igneous rocks, we can construct curves to show the relation between the concentration of an alkali element X^+ and the Cl^- concentration of geothermal waters (Figs.3 and 4). It is assumed that the concentrations of Cs and Rb in feldspars range from 10^{-3} to 10^{-4} wt.% and from 10^{-1} to 10^{-2} wt.%, respectively. The exchange reactions between solution and feldspars for Cs and Rb were studied by Lagasche and Sabatier (1973) and Volfinger (1975). The partition coefficients below 400° C have not yet been determined. Therefore, using the value for 400° C by Volfinger (1975) and the relation between the K^+ and Cl^- concentrations shown in Fig.2, the relation between the alkali element (Rb^+ and Cs^+) concentration and Cl^- concentration was derived. It is apparent from Figs. 3 and 4 that a linear relation with slope approximately +1 exists between the alkali-element concentration and the Cl^- concentration. The partition coefficient for Li has not yet been determined, but it is predicted that on a $\log(m_{Li^+}) - \log(m_{Cl^-})$ (Fig.5) diagram a slope of approximately +1 would also be obtained, if the exchange reaction of Na and Li between solution and feldspar is in equilibrium.

H^+ concentration. Muscovite and quartz are commonly present in geothermal areas. If these minerals are saturated with geothermal waters, the following reaction can be written:

$$3\ \text{K-feldspar} + 2H^+ \rightleftharpoons \text{muscovite} + 6\ \text{quartz} + 2\ K^+ \qquad (7)$$

Using the equilibrium constant for reaction (7) by Helgeson (1969) and eq. 4, the relation between pH and Cl^- concentration can be derived (Fig.6). The line shown in Fig.6 has a slope of approximately −1 and indicates that with increasing Cl^- concentration the pH of the geothermal water decreases.

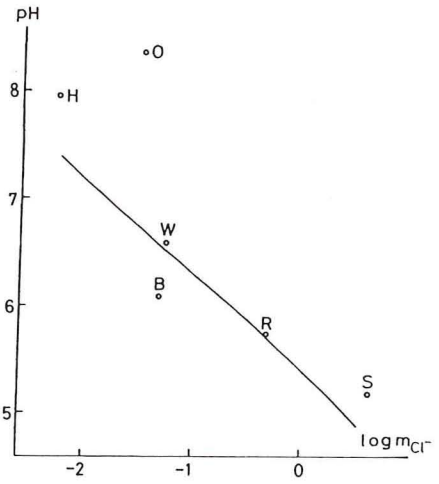

Fig.6. Relation between the pH and Cl^- concentration of geothermal waters. The *solid line* indicates the albite—K-feldspar—muscovite—quartz—solution equilibrium at 250° C. For symbols used see caption to Fig.1.

Ca^{2+} concentration. If calcite is saturated with geothermal waters, the following reaction is written:

$$CaCO_3 + 2H^+ \rightleftharpoons Ca^{2+} + H_2CO_3 \quad (8)$$

Combining the equilibrium relation for reaction (8) and the relation between pH and the Cl^- concentration derived already, we can derive the dependence of Ca^{2+} concentration on Cl^- concentration (Fig.7). At constant temperature and activity of H_2CO_3, $\log(m_{Ca^{2+}})$ plots linearly as a function of the logarithmic concentration of Cl^- with a slope of about +2. The validity of the assumption of constant activity of H_2CO_3 is not certain as the concentration of this species changes not only with variations in the acidity but also with variations in the oxidation—reduction state of the solution. In the reduced condition, for example, H_2CO_3 would be converted to reduced C species such as aqueous CH_4. Generally, in geothermal systems, H_2CO_3 concentration changes widely. Therefore, the curves for the equilibrium above mentioned are constructed under the different H_2CO_3 activities.

The saturation curve for anhydrite was constructed considering the following reaction:

$$CaSO_4 + Na^+ \rightleftharpoons Ca^{2+} + NaSO_4^- \quad (9)$$

From this equilibrium relation and eq. 2, we obtain:

$$\log(m_{Ca^{2+}}) = \log(m_{Cl^-}) + \log(c_3) \quad (10)$$

in which $c_3 = (\gamma_{Na^+} \cdot K_9)/(m_{NaSO_4^-} \cdot \gamma_{NaSO_4^-} \cdot \gamma_{NaSO_4^-} \cdot \gamma_{Ca^{2+}})$

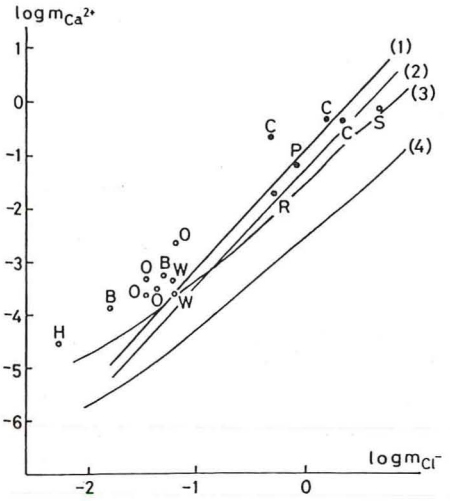

Fig.7. Relation between the Ca^{2+} and Cl^- concentrations of geothermal waters and inclusion fluids. *Solid lines* indicate: (*1*) albite—K-feldspar—muscovite—quartz—calcite—solution equilibrium at $a_{H_2CO_3} = 10^{-2.5}$; (*2*) albite—K-feldspar—muscovite—quartz—calcite—solution equilibrium at $a_{H_2CO_3} = 10^{-2}$; (*3*) anhydrite—solution at ΣS_0 (total dissolved sulfate concentration) = 10^{-3}; and (*4*) anhydrite—solution equilibrium at $\Sigma S_0 = 10^{-2}$. For symbols used see caption to Fig.1.

The anhydrite saturation curve is drawn at constant total sulfate concentration and temperature (Fig.7). However, in a geothermal system, total sulfate concentration changes with the variations in some physicochemical parameters. For example, oxygen fugacity is important for controlling total sulfate concentration. In the salinity condition considered here, $NaSO_4^-$ is predominant among oxidized S species. Thermochemical data for the oxidized S species are from Helgeson (1969) and Ohmoto (1972) and for anhydrite from Helgeson (1969). The equilibrium constant for the dissociation reaction $NaSO_4^- \rightleftharpoons Na^+ + SO_4^{2-}$ is assumed to be the same as that for the dissociation reaction $KSO_4^- \rightleftharpoons K^+ + SO_4^{2-}$. The equilibrium curves for anhydrite are also plotted for the different total sulfate concentrations, because it also changes widely in geothermal systems. Eq.10 predicts that the slope is about +1 on a $\log(m_{Ca^{2+}}) - \log(m_{Cl^-})$ diagram. However, the slope shown in Fig.7 is different from +1. This is due to the effects of activity coefficients of γ_{Na^+}, $\gamma_{NaSO_4^-}$ and $\gamma_{Ca^{2+}}$ in eq. 10.

Mg^{2+} concentration. Chlorite commonly coexists with albite, K-feldspar, muscovite and quartz. The equilibrium relation among these minerals and solution is given in Fig.8. It is seen that $\log(m_{Mg^{2+}})$ plots linearly as a function of $\log(m_{Cl^-})$ with a slope of about +2. The thermochemical data for Mg-chlorite were taken from Helgeson (1969). Generally, considerable amounts of Fe are contained in chlorite; the Fe content of chlorite varies with temperature, oxygen and sulfur fugacities, if it is in equilibrium with Fe-oxides and -sulfides. Therefore, the Mg^{2+} concentration in the solution will vary not only as a function of the Cl^- concentration and temperature but also with other variables such as oxygen and sulfur fugacities. If these

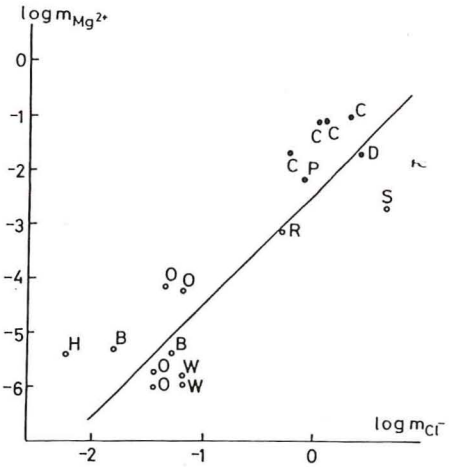

Fig.8. Relation between the Mg^{2+} and Cl^- concentrations of geothermal waters. The *solid line* indicates albite—K-feldspar—muscovite—quartz—Mg-chlorite—solution equilibrium at 250° C. For symbols used see caption to Fig.1.

variables change considerably in geothermal systems, the Mg^{2+} concentration deviates from the equilibrium curve in Fig.8. In the present discussion the activity of Mg-chlorite is taken to be unity.

Sr^{2+} concentration. The dependence of the Sr^{2+} concentration on the Cl^- concentration is nearly identical to that determined for the Ca^{2+} ion. If the Sr^{2+} concentration is controlled by carbonate or silicate equilibria, the equilibrium line should have a slope of approximately +2 (Fig.9). However, if instead of these equilibria, the Sr^{2+} concentration is controlled by sulfate

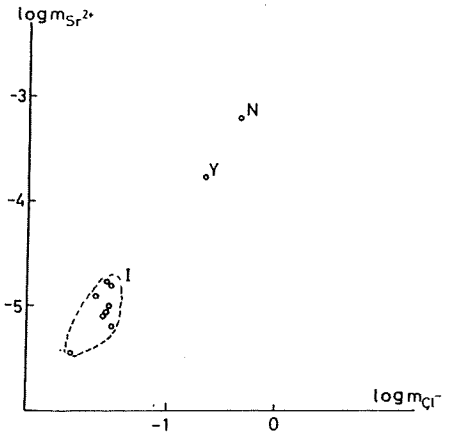

Fig.9. Relation between the Sr^{2+} and Cl^- concentrations of Japanese hot springs. *Abbreviations*: *Y* = Yudonoyama (Ichikuni et al., 1974); *N* = Naganuma (Ichikuni et al., 1974); *I* = hot springs in Izu (Araki, 1974).

mineral, the dependence of the Sr^{2+} on the Cl^- concentrations is derived from the following reaction:

$$SrSO_4^{sulfate} + Na^+ \rightleftharpoons Sr^{2+} + NaSO_4^- \qquad (10)$$

in which $SrSO_4^{sulfate}$ is the $SrSO_4$ component in sulfate minerals such as barite and anhydrite.

The slope of the curve showing this equilibrium is considered to be about +1 at constant temperature and total sulfate concentration. However, if the effect of activity coefficients (γ_{Na^+},$\gamma_{Sr^{2+}}$,$\gamma_{NaSO_4^-}$) is large, the slope differs from +1 as same as in the case of the Ca^{2+}—Cl^- relation for the anhydrite—solution equilibrium. Moreover, because the $NaSO_4^-$ is not always predominant among oxidized S species and constant, it is considered that the relation between Sr^{2+} and Cl^- is complicated.

Ba^{2+} concentration. If the Ba^{2+} concentration in solution is controlled by the Ba content of feldspars, a line with a slope of approximately +2 is obtained on a logarithmic Ba^{2+}—Cl^- concentration diagram at constant

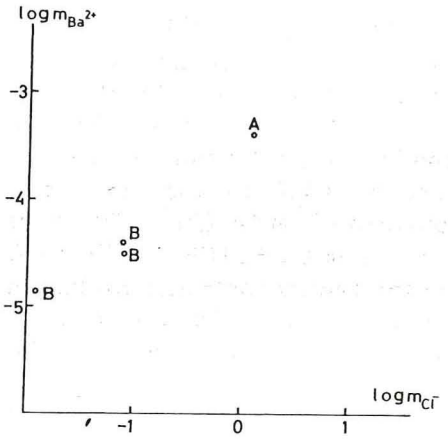

Fig.10. Relation between the Ba^{2+} and Cl^- concentrations of Japanese hot springs. *Abbreviations*: *A* = Arima (Ikeda, 1955); *B* = Beppu (Kawakami, 1966).

temperature (Fig.10). However, if the Ba^{2+} concentration is controlled by the solubility of barite, the dependence of the Ba^{2+} concentration on the Cl^- concentration is derived from the following reaction:

$$BaSO_4 + Na^+ \rightleftharpoons Ba^{2+} + NaSO_4^- \quad (11)$$

The slope of the barite saturation curve is nearly +1 in a $\log(m_{Ba^{2+}})$ — $\log(m_{Cl^-})$ diagram at constant temperature and $m_{NaSO_4^-}$ in the predominance region of $NaSO_4^-$ among oxidized S species, if the effect of ionic activity coefficients is not large.

Relation between the concentration of elements and that of Cl^- in divalent cation and Cl^- dominant solutions

As can be seen in Fig.1, 7 and 11 the divalent cation concentration such as the Ca^{2+} concentration exceeds the monovalent cation concentration such as the Na^+ concentration in high Cl^- concentration ranges. The slope of the $\log(m_{Ca^{2+}})$ line (line *1* in Fig.11) is steeper than that of the $\log(m_{Na^+})$ line (line *2* in Fig.11) and they intersect one another if divalent cations such as Ca^{2+} are the predominant cations and if Cl^- is the most abundant anion, and the condition of electroneutrality is approximated by, for example:

$$2(m_{Ca^{2+}}) = (m_{Cl^-}) \quad (12)$$

This relation is shown in Fig.11 as line *3*. from eq. 12 and the assumption of chemical equilibrium among calcite, albite, muscovite, K-feldspar and solution, we obtain the relation:

$$\log(m_{Na^+}) = 0.5\log(m_{Cl^-}) + \log(c_5) \quad (13)$$

in which the term c_5 is a function of temperature, activity of H_2CO_3 and ionic strength.

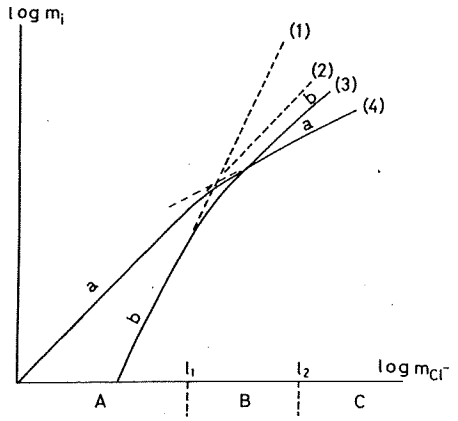

Fig.11. Schematic diagram showing the relations between the dominant monovalent cation (such as Na^+) and Cl^- concentrations and the dominant divalent cation (such as Ca^{2+}) and Cl^- concentrations. The *lines* in the figure are: (*1*) the equilibrium relation for albite—K-feldspar—muscovite—quartz—calcite—solution at constant temperature and activity of H_2CO_3; (*2*) the condition of electroneutrality approximated by the relation $m_{Na^+} = m_{Cl^-}$; (*3*) the condition of electroneutrality approximated by the relation $2m_{Ca^{2+}} = m_{Cl^-}$; and (*4*) the equilibrium relation for albite—K-feldspar—muscovite—calcite—quartz—solution at constant temperature and activity of H_2CO_3. *Solid lines a* and *b* show the relations between the Na^+ and Cl^- and the Ca^{2+} and Cl^- concentrations respectively in natural geothermal systems. The regions *A*, *B* and *C* are low-m_{Cl^-}, intermediate-m_{Cl^-} and high-m_{Cl^-} regions.

The slope of the line defined by eq. 13 on the $\log(m_{ci})$—$\log(m_{Cl^-})$ diagram is approximately +0.5 (line *4* in Fig.11) if the term such as c_5 is constant. Data for other monovalent cations will also fall on lines having slopes of +0.5 (Figs.11 and 12). On the contrary, it can be shown that the slope of the equilibrium curve for divalent cations is approximately +1 (Figs.11 and 13).

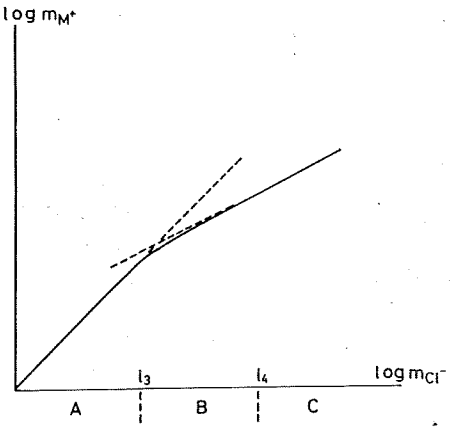

Fig.12. Schematic representation showing the relation of alkali-element concentrations to the Cl^- concentration (*solid line*). *A* = low-m_{Cl^-} region; *B* = intermediate-m_{Cl^-} region; and *C* = high-m_{Cl^-} region.

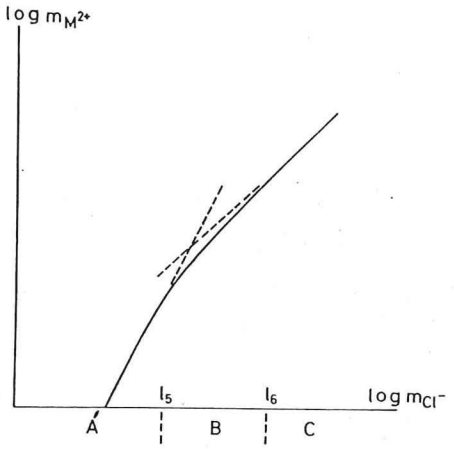

Fig.13. Schematic representation showing the relation of alkali-earth-element concentrations to the Cl^- concentration (*solid line*). *A* = low-m_{Cl^-} region; *B* = intermediate-m_{Cl^-} region; and *C* = high-m_{Cl^-} region.

Schematic representations illustrating the relation between the molalities of the cations and Cl^- are presented in Figs.11—13. In the low-m_{Cl^-} region (*A*), where a given monovalent cation predominates among cations, the slopes for divalent and monovalent cations are approximately +2 and +1, respectively. In the intermediate-m_{Cl^-} region (*B*) where both a given divalent cation and a given monovalent cation predominate, the slope for a divalent cation lies between +1 and +2 and for a monovalent cation between +0.5 and +1. In the high-m_{Cl^-} region (*C*), one of the divalent cation such as Ca^{2+} predominates and the slope of the curve is +1 for a divalent cation and +0.5 for a monovalent cation.

COMPARISON OF THEORETICAL CONSIDERATIONS WITH ANALYTICAL DATA ON CHLORIDE-RICH GEOTHERMAL WATERS AND INCLUSION FLUIDS

In order to compare the theoretical consideration with analytical data, the geothermal waters and areas have to satisfy the following conditions: (1) Cl^- is dominant compared with the other anions such as HCO_3^-, $NaSO_4^-$ and SO_4^{2-}; (2) the temperature is relatively high (200—300°C); (3) analytical data represent a deep-seated condition; and (4) alteration minerals considered here are found. The geothermal areas satisfying these conditions are scarce and these are Salton Sea (U.S.A.), Reykjanes (Iceland), Wairakei (New Zealand), Broadland (New Zealand), Otake (Japan) and Hveragerdi (Iceland). In addition to the geothermal waters chemical analytical data on inclusion fluids in the hydrothermal minerals from Climax, Darwin and Providencia deposits are also plotted on the $\log(m_{ci}) - \log(m_{Cl^-})$ diagrams. As analytical data for Sr^{2+} and Ba^{2+} in high-temperature geothermal waters and inclusion fluids are few, data for these elements from low-temperature (50—100°C) Japanese hot springs were used.

Na^+ concentration. Both the theoretical curve and the curve fitted to the analytical data have slopes of approximately +1 on the $\log(m_{Na^+})$—$\log(m_{Cl^-})$ diagram (Fig.1).

K^+ concentration. The natural data generally satisfy the theoretical curve (Fig.2). It seems likely that the slope satisfying the natural data is about +1.

Cs^+ concentration. The slope of the curve defined by the data from geothermal areas is approximately +1 and seems to be consistent with the theoretical curve constructed when assuming equilibrium between solution and feldspars (Fig.3).

Rb^+ concentration. Natural data for Rb^+ approximate the slope of the calculated curve (Fig.4).

Li^+ concentration. The curve fitted to the analytical data for Li has a slope of approximately +1 on the $\log(m_{Li^+})$—$\log(m_{Cl^-})$ diagram (Fig.5).

H^+ concentration. Data for the pH of geothermal waters were obtained at room temperature. The pH is observed to decrease with increasing Cl^- concentration, and seems to be consistent with the theoretical curve, although the data vary more widely than for the alkali elements (Fig.6). This more wide variation would be due to steam release. The pH values of Broadland, Wairakei, and Hveragerdi were corrected for high temperature by Ellis (1967), but the other data plotted are not corrected.

Ca^{2+} concentration. Data for Ca analyses plot close to the theoretical curve (Fig.7). This would be due to the reaction between the solution and the assemblage of albite, K-feldspar, muscovite, calcite, anhydrite and quartz. The data appear to vary more widely than was observed for the alkali elements. This may be a result from the variation of CO_2 and $NaSO_4^-$ concentrations in geothermal waters. The slope of the curve fitted to the natural data seems to be closer to +2 than +1.

Mg^{2+} concentration. Although the data for Mg^{2+} vary quite widely, the concentration of this cation does appear to increase with increasing Cl^- concentration with a slope of about +2 and the data plot close to the theoretical curve (Fig.8).

Sr^{2+} concentration. The correlation between the Sr^{2+} and Cl^- concentrations of several Japanese hot springs is shown in Fig.9. In these hot springs the ratio divalent cation/monovalent cation is less than 1. This means that the solution lies in the low-m_{Cl^-} or intermediate-m_{Cl^-} region in Fig.11. Although data are scarce, the slope of the curve fitted to the natural data seems to be about +1. Based on the theoretical considerations mentioned already and on

analytical data, there are two possible interpretations of the natural data. One is that the Cl^- concentration falls within the intermediate range (*B*) schematically represented in Fig.13. The positions of the boundaries between the low, intermediate and high Cl^- concentration ranges, l_1 and l_2 in Fig.11, l_3 and l_4 in Fig.12, l_5 and l_6 in Fig.13, respectively, will shift with changes in temperature. It is felt that the boundaries will shift to relatively lower Cl^- concentrations with a decrease in temperature. The other is that Sr^{2+} is controlled by sulfate mineral.

Ba^{2+} concentration. The relatively few data available for Ba^{2+} are plotted in Fig.10. In these hot springs, the divalent cation/monovalent cation ratio is also less than 1. These few data points, nevertheless, appear to define a line with a slope closer to +1 than +2, as was observed for the case of Sr^{2+}. The same interpretation can be given for Ba^{2+} as was used for Sr^{2+}; it may be interpreted that: (1) the divalent cation/monovalent cation ratio is relatively large, or (2) Sr^{2+} is controlled by the sulfate mineral.

CONCLUSIONS

If the chemical composition of the solution is buffered by the common mineral assemblage with which it is in contact, and if Cl^- is the dominant anion in the solution, it is theoretically considered that:

(1) The concentrations of alkali and alkali-earth elements will increase with increasing Cl^- concentrations, with slopes of about +1 and +2, respectively, in monovalent cation (such as Na^+) predominant solutions.

(2) In solutions with high Cl^- concentrations, the slopes for divalent cations (such as Ca^{2+}) on $\log(m_{Ci})$—$\log(m_{Cl^-})$ plots exceed those for monovalent cations (such as Na^+). The slope for monovalent cations is approximately +0.5 and for divalent cations approximately +1.

(3) In solutions with intermediate Cl^- concentrations in which both monovalent and divalent cations are dominant, the slope lies between that in the high- and the low-Cl^- concentration ranges.

Theoretical curves showing the equilibrium between solution and the assemblage albite—K-feldspar—muscovite—quartz—chlorite and a Ca-phase (calcite or anhydrite) are drawn on logarithmic cation—Cl^- concentration diagram, assuming that: (1) temperature is constant; (2) Cl^- is the dominant anion; and (3) Na^+ concentration is equal to Cl^- concentration. Analytical data (Na^+, K^+, Cs^+, Rb^+, Li^+, H^+, Ca^{2+}, Mg^{2+}) from some geothermal waters and inclusion fluids closely approximate the theoretically predicted curves. The analytical data for Sr^{2+} and Ba^{2+} from low-temperature (50—100°C) Japanese hot springs define lines with slopes closer to +1 than +2, although data are scarce. One possible interpretation is that the solution has an intermediate Cl^- concentration and that the divalent cation/monovalent cation ratio increases at low temperatures relative to high temperatures. The other interpretation is that these concentrations are controlled by the sulfate mineral.

In order to more strictly interpret the cation concentrations in natural hydrothermal solutions, we have to take into account the following effects in the future: (1) the other anion concentrations (such as HCO_3^-, SO_4^{2-}, $NaSO_4^-$, etc.); (2) the oxygen fugacity; (3) the activity coefficients of ionic and neutral species; (4) the solid solution of minerals; and (5) temperature dependence of the mineral—solution equilibrium.

ACKNOWLEDGEMENTS

The author wishes to express his appreciation to Prof. J.T. Iiyama of the University of Tokyo and to Dr. Y. Kajiwara of Tsukuba University for their discussions and critical reading of the manuscript.

He is indebted to Mr. C.W. Farrell of Harvard University for improvement of the English in the original manuscript.

He also wishes to thank Prof. M. Ichikuni of Tohoku University for helping to assemble the analytical data on the Japanese hot springs.

REFERENCES

Araki, T., 1974. The minor component of calcium carbonate sediments precipitated from the hydrothermal well waters in the Izu District, Shizuoka Prefecture. Onsenkagaku, 25: 20—25. (in Japanese).

Björnsson, S., Arnorsson, S. and Tomasson, J., 1970. Exploration of the Reykjanes thermal brine area. Geothermics Spec. Iss., 2: 1640—1650.

Browne, P.R.L. and Ellis, A.J., 1970. The Ohaki—Broadlands hydrothermal area, New Zealand — Mineralogy and related geochemistry. Am. J. Sci., 269: 97—137.

Ellis, A.J., 1967. The chemistry of some explored geothermal systems. In: H.L. Barnes (Editor), Geochemistry of Hydrothermal Ore Deposits. Holt, Rinehart and Winston, New York, N.Y., pp. 465—514.

Ellis, A.J., 1969. Present-day hydrothermal systems and mineral deposition. 9th Commonw. Min. Metall. Congr. Min. Pet. Geol. Sect., Pap. 7, 30 pp.

Ellis, A.J., 1970. Quantitative interpretation of chemical characteristics of hydrothermal systems. Geothermics Spec. Iss., 2: 516—528.

Fournier, R.O. and Truesdell, A.H., 1973. Empirical Na—K—Ca geothermometer for natural waters. Geochim. Cosmochim. Acta, 37: 1255—1275.

Garrels, R.M. and Christ, C.L., 1965. Solutions, Minerals, and Equilibria. Harper and Row, New York, N.Y. 450 pp.

Hall, W.E., Friedman, I. and Nash, J.T., 1974. Fluid inclusion and light stable isotope study of the Climax molybdenum deposits, Colorado. Econ. Geol., 69: 884—901.

Hayashi, M., 1973. Hydrothermal alteration in the Otake geothermal area, Kyushu. Jinetsu, 10: 9—46.

Hayashida, T. and Ejima, Y., 1970. Development of Otake geothermal field. Geothermics (Spec. Iss.), 2: 208—220.

Helgeson, H.C., 1969. Thermodynamics of hydrothermal systems at elevated temperatures and pressure. Am. J. Sci., 267: 729—804.

Hemley, J.J., 1967. Aqueous Na/K ratios in the systems K_2O—Na_2O—Al_2O_3—SiO_2—H_2O. Program, 1967 Annu. Meet., Geol. Soc. Am., New Orleans, La., pp. 94—95.

Ichikuni, M., Suzuki, R. and Kato, T., 1974. Chemical characteristic of saline springs. Onsenkagaku, 25: 21—25 (in Japanese).

Iiyama, J.T., 1965. Influence des anions sur les équilibres d'ions Na—K dans la série muscovite—paragonite. Bull. Soc. Fr. Mineral. Cristallogr., 87: 532—541.

Ikeda, N., 1955. Arima thermal springs, (3): Tenmanguno-yu, (1). Major constituents, rare alkalis, Sr, Ba. J. Chem. Soc. Jpn., 76: 716—721. (in Japanese).
Kawakami, H., 1966. Chemical observation on the Beppu hot springs — particularly on the trace elements,. Onsenkagaku, 17: 58—82 (in Japanese).
Keith, T.E.C., Muffler, L.J.P. and Cremer, M., 1968. Hydrothermal epidote from the Salton Sea geothermal field, California. Am. Mineral., 53: 1635—1644.
Koga, A., 1970. Geochemistry of the waters discharged from drillholes in the Otake and Hachobaru areas. Geothermics (Spec. Iss.), 2: 1422—1425.
Lagasche, M. and Sabatier, G., 1973. Distribution des éléments Na, K, Rb et Cs à l'état de trace entre feldspaths alcalins et solutions hydrothermales à 650° C, 1 kbar; données expérimentales et interpretation thermodynamique. Geochim. Cosmochim. Acta, 37: 2617—2640.
Mahon, W.A.J. and Finlayson, J.B., 1972. The chemistry of the Broadlands geothermal area, New Zealand. Am. J. Sci., 272: 48—68.
Muffler, L.J.P. and White, D.E., 1969. Active metamorphism of upper Cenozoic sediments in the Salton Sea geothermal field and Salton through, southeastern California. Geol. Soc. Am. Bull., 80: 157—182.
Ohmoto, H., 1972. Systematics of sulfur and carbon isotopes in hydrothermal ore deposits. Econ. Geol., 67: 551—578.
Orville, P.N., 1963. Alkali ion exchange between vapor and feldspar phases. Am. J. Sci., 261: 201—237.
Rye, R.O. and Haffty, J., 1969. Chemical composition of the hydrothermal fluids responsible for the lead—zinc deposits at Providencia, Zacatecas, Mexico. Econ. Geol., 64: 629—643.
Rye, R.O., Hall, W.E. and Ohmoto, H., 1974. Carbon, hydrogen, oxygen, and sulfur isotope study of the Darwin lead—silver—zinc deposit, southern California. Econ. Geol., 69: 468—481.
Shikazono, N., 1976. Thermodynamic interpretation of Na—K—Ca geothermometer in the natural water systems. Geochem. J., 10: 47—50.
Sigvaldason, G.E., 1959. Mineralogische Untersuchungen über Gesteinszersetzung durch postvulkanische Aktivität in Island. Beitr. Mineral. Petrogr., 6: 405—426.
Sigvaldason, G.E., 1967. Epidote and related minerals in two deep geothermal drill holes, Reykjavik and Hveragerdi, Iceland. U.S. Geol. Surv., Prof. Pap., 450E: 77—79.
Steiner, A., 1953. Hydrothermal rock alteration at Wairakei, New Zealand. Econ. Geol., 48: 1—13.
Steiner, A., 1968. Clay minerals in hydrothermally altered rocks at Wairakei, New Zealand. Clays Clay Miner., 16: 193—213.
Steiner, A., 1970. Genesis of hydrothermal K-feldspar (adularia) in an active geothermal environment at Wairakei, New Zealand. Mineral. Mag., 37: 916—922.
Tomasson, J. and Kristmannsdóttir, H., 1972. High temperature alteration minerals and thermal brines, Reykjanes, Iceland. Contrib. Mineral. Petrol., 36: 123—134.
Volfinger, M., 1975. Effect de la température sur les distributions de Na, Rb et Cs entre la sanidine, la muscovite, la phlogopite et une solution hydrothermale sous une pression de 1 kbar. Geochim. Cosmochim. Acta, 40: 267—282.
White, D.E., 1965. Saline waters of sedimentary rocks. In: Fluids in Subsurface Environment — A Symposium. Am. Assoc. Pet. Geol., Mem., 4: 342—366.
Yamasaki, T., Matsumoto, Y. and Hayashi, M., 1968. Geology of the Otake geothermal area, Kujū Volcano Group, Kyūshū — with preliminary note of hydrothermal alteration. Jinetsu., 12—23 (in Japanese).